Journal of the Serbian Chemical Society
JSCS@tmf.bg.ac.rs • www.shd.org.rs/JSCS
J. Serb. Chem. Soc. *88* (12) 1205–1222 (2023)
JSCS–5690
Original scientific paper
Published 19 December 2023

Iron(III) complexes with ditopic macrocycles bearing crown-ether and bis(salicylidene) isothiosemicarbazide moieties

VLADIMIR B. ARION[1]*, OLEG PALAMARCIUC[2], SERGIU SHOVA[3], GHENADIE NOVITCHI[4] and PETER RAPTA[5]

[1]University of Vienna, Institute of Inorganic Chemistry, Währinger Strasse 42, A-1090 Vienna, Austria, [2]Moldova State University, A. Mateevici Street 60, MD-2009 Chisinau, Republic of Moldova, [3]Inorganic Polymers Department, "Petru Poni" Institute of Macromolecular Chemistry, Aleea Gr. Ghica Voda 41 A, Iasi 700487, Romania, [4]CNRS-LNCMI, 38042 Grenoble Cedex, France and [5]Institute of Physical Chemistry and Chemical Physics, Faculty of Chemical and Food Technology, Slovak University of Technology in Bratislava, Radlinského 9, SK-81237 Bratislava, Slovakia

(Received 7 June, revised 4 July, accepted 8 September 2023)

Abstract: The main aims of this work were the synthesis and characterization of iron(III) complexes with a ditopic ligand H_2L consisting of a bis(salicylidene)isothiosemicarbazide moiety with a N_2O_2 binding site and a crown-ether (O_6) moiety. A series of high-spin iron(III) complexes, *i.e.*, $[Fe^{III}LClBa(CH_3OH)(H_2O)_{0.5}(ZnCl_4)]$ (**1**), $[Fe^{III}LCl]$ (**2**), $[Fe^{III}L(N_3)]$ (**3**) and $[(Fe^{III}L)_2O]$ (**4**), were synthesized. The complexes were characterized by mass spectrometry, IR and UV–Vis spectroscopy, variable temperature (VT) magnetic susceptibility measurements, Mössbauer spectroscopy, single crystal X-ray diffraction and cyclic voltammetry.

Keywords: iron(III); bi-compartmental ligand; Mössbauer; magnetism.

INTRODUCTION

Bi-compartmental ligands with both a salen moiety for "soft" metal cations and a crown ether moiety for "hard" metal cations were reported 35 years ago by Reinhoudt *et al.*[1,2] Nickel(II), copper(II) and zinc(II) complexes, with both metal-free crown ether cavity and alkali- and alkaline-earth cations located in crown ether moiety in close proximity to first-row transition metal, were synthesized and comprehensively characterized by spectroscopic, electrochemical and X-ray diffraction methods. The relative simplicity of the general approach for their assembly[3,4] has permitted the building up of a large number of such systems, systematically modifying the structure of each binding site. The nature of

* Corresponding author. E-mail: vladimir.arion@univie.ac.at
https://doi.org/10.2298/JSC230607065A

the metal-binding sites in these systems is so different that hard alkali, alkaline-earth or lanthanide metal cations and softer transition metal ions can be bound simultaneously and located in close proximity to each other within the same macrocycle. Generally, these bi-compartmental ligands are assembled in the presence of a metal ion template. Barium(II) proved to be the most suitable template for the synthesis of macrocyclic salen- and salophen-crown ethers from the appropriate building blocks.[5–7] This behavior is not surprising as Ba^{2+} has been successfully used in the synthesis of a number of crown ethers.[8] The template role of barium(II) is predominantly conformational. By coordination of the polyoxyethylene-containing building blocks to barium(II) the terminal 2-hydroxybenzaldehyde groups are held in close proximity. Under such conditions the cyclization of the 1+1 open-chain condensation product occurs inevitably at the next step of the template process. This pathway is favored over the intermolecular one that leads to polymerization. Another important reason for using Ba^{2+} as template is the possibility to remove it easily from the final template product by treatment with SO_4^{2-}. Even though first attempts to use K^+, Rb^+ or Cs^+ as templates failed,[1] later it was shown that K^+, which has very close ionic radius to that of Ba^{2+}, can also serve as a template for assembly of heterometallic systems.[9]

By using Ba^{2+} as template ditopic macrocycles based on bis(salicylidene)-isothiosemicarbazide or acetamidrazone unit and crown-ether moiety were assembled and isolated as Ni(II)–Ba(II), Cu(II)–Ba(II), Zn(II)–Ba(II), VO(II)–Ba(II) and Cu(II)–Gd(III) heterodinuclear complexes[10–14] as shown in Scheme 1.

The "complex formation" behavior of nickel(II) complexes with alkali and alkaline earth metal ions was investigated by UV–Vis spectroscopy and calorimetric techniques and revealed building of 1:2 metal-nickel(II) macrocycle associates.[15] In addition, electrochemical recognition properties of first raw transition metal macrocycles vs alkali and alkaline earth metal cations, ammonium cation and protonated dopamine were studied.[16]

Herein we report the synthesis of iron(III) complexes with a bi-compartmental macrocyclic system H_2L, namely $[Fe^{III}LClBa(CH_3OH)(H_2O)_{0.5}(ZnCl_4)]$ (**1**), $[Fe^{III}LCl]$ (**2**), $[Fe^{III}L(N_3)]$ (**3**) and $[(Fe^{III}L)_2O]$ (**4**) as shown in Scheme 2, their characterization by single crystal X-ray diffraction, spectroscopic techniques (UV−Vis, IR), ESI mass spectrometry, magnetochemistry, Mössbauer spectroscopy and cyclic voltammetry. As the interstitial solvent or its amount in the isolated bulk samples and single crystals investigated by X-ray crystallography (vide infra) differ, the numbering of the complexes in the following discussion will not include the co-crystallized solvent.

EXPERIMENTAL

All starting materials and solvents were purchased from Aldrich and used without further purification.

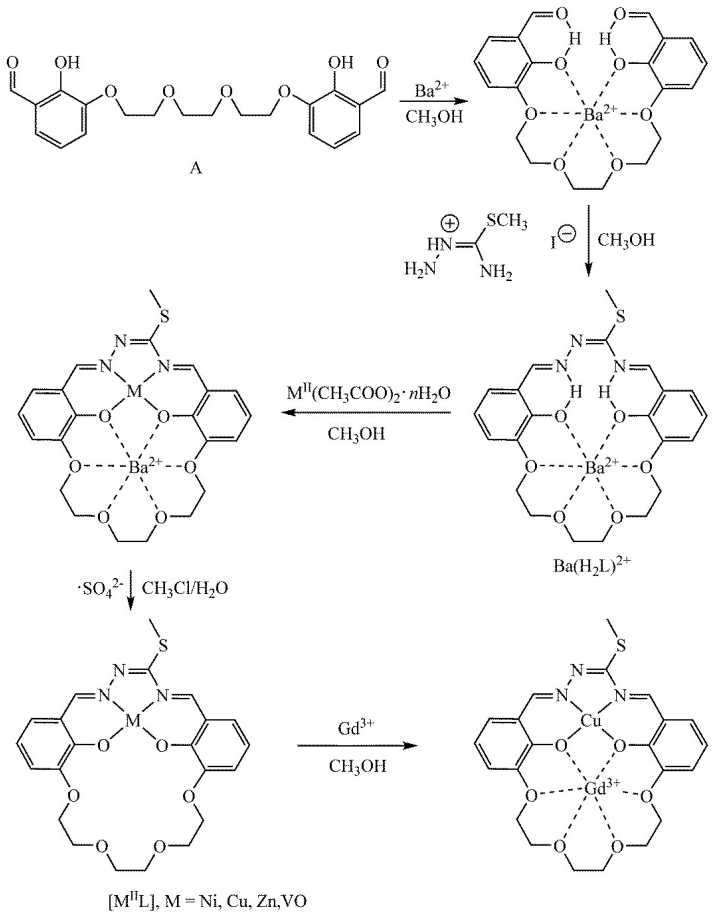

Scheme 1. Synthetic pathway to the heteronuclear bis(salicylidene)isothiosemicarbazide--crown ether macrocycle H_2L. The last transformation was reported for M = Cu.[14]

Synthesis of $[Fe^{III}LClBa(CH_3OH)(H_2O)_{0.5}(ZnCl_4)]\cdot CH_3OH$ (**1**$\cdot CH_3OH$)

To $[ZnLIBa(CF_3SO_3)CH_3OH]_2\cdot 0.5H_2O$[11] (0.7 g, 0.36 mmol) in CH_3OH (20 ml) was added $FeCl_3\cdot 6H_2O$ (0.9 g, 3.3 mmol) in methanol (15 ml). The black crystals formed were isolated by filtration, washed with cold methanol and diethyl ether and dried in air. Yield: 0.45 g (64 %).

Synthesis of $[Fe^{III}LCl]\cdot CH_2Cl_2\ 0.5H_2O$ (**2**$\cdot CH_2Cl_2\ 0.5H_2O$)

A suspension of $[Fe^{III}LClBa(CH_3OH)(H_2O)_{0.5}(ZnCl_4)]\cdot CH_3OH$ (1.0 g, 1.1 mmol) in CH_2Cl_2 (250 ml) was stirred with a solution of guanidinium sulfate (3.0 g) in water (150 ml) for 30 min. The resulting colored organic layer was separated off and dried over $MgSO_4$. The solvent was removed to ~20 ml by evaporation under a reduced pressure and the product

precipitated with pentane. X-ray diffraction quality single crystals were grown from CH_2Cl_2. Yield: 0.55 g (82 %).

*Synthesis of [$Fe^{III}L(N_3)$] (**3**)*

A mixture of [Fe^{III}LCl]·CH_2Cl_2·0.5H_2O (0.55 g, 0.86 mmol) and NaN_3 (0.51 g, 22.2 mmol) in CH_3OH was stirred for 1 h. The solvent was then evaporated under reduced pressure, the residue re-dissolved in CH_2Cl_2 (50 ml) and the solution formed filtered. The solvent was removed under reduced pressure up to *ca*. 10 ml and the product precipitated with pentane. Yield: 0.44 g (94 %).

*Synthesis of [($Fe^{III}L)_2O$]·H_2O (**4**·H_2O)*

Method a. To green-brown solution of [Fe^{III}LCl]·CH_2Cl_2·0.5H_2O (0.5 g, 0.78 mmol) in methanol (170 ml) at 60 °C was added triethylamine (0.22 ml, 1.56 mmol). The red solution generated was allowed to stand at room temperature for 48 h. The product was isolated by filtration, washed with methanol and dried in vacuo. Yield: 0.30 g (79 %). X-ray diffraction quality single crystals were grown by slow diffusion of pentane into solution of the product (14 mg) in chloroform (15 ml).

Method b. To a red-brown solution of [Fe^{III}LCl]·CH_2Cl_2·0.5H_2O (0.2 g, 0.31 mmol) in CH_2Cl_2 (35 ml) was added a solution of KOH (0.02 g, 0.37 mmol) in water (35 ml). The mixture was stirred at room temperature for 105 min. After separation of the two phases the organic one was dried over $MgSO_4$. Slow addition of pentane to the solution produced a small amount of red microcrystals, which were separated by filtration, washed with pentane and dried in air. Yield: 0.02 g (13 %). The IR spectrum of the isolated product was identical with that synthesized by method a.

Analytical and spectral data are given in Supplementary material to this paper.

Crystallographic structure determination

The measurements were performed on Siemens SMART (**1**·H_2O) and **2**·CH_2Cl_2·0.5H_2O) and Bruker D8 Venture (**4**·$CHCl_3$) diffractometers. Crystal data, data collection parameters, and structure refinement details are given in Table S-I of the Supplementary material. The structures were solved by direct methods and refined by full matrix least-squares techniques. Non-hydrogen atoms were refined with anisotropic displacement parameters. The positional parameters of the atoms belonging to disordered fragments were modeled by using PART, DFIX and SADI tools of SHELXL-2014 program. The *S*-methylisothiosemicarbazide fragment was found to be disordered over two positions with the refined occupancy factors 0.59:0.41, 0.58:0.42 (0.66:0.33) and 0.74:0.26 (0.75:0.25) for **1**·H_2O, **2**·CH_2Cl_2·0.5H_2O and **4**·$CHCl_3$, respectively. In the crystal of **1**·H_2O, $ZnCl_4^{2-}$ is also disordered, wherein two chlorido coligands occupy unique positions, while the other two are equally distributed between the two orientations. The disorder was modeled similarly in the crown-ether moieties in **2**·CH_2Cl_2·0.5H_2O and **4**·$CHCl_3$. It turned out, that one of two independent crown-ether moieties is fully disordered (for **2**·CH_2Cl_2·0.5H_2O) or partially disordered (**4**·$CHCl_3$) over two positions with 0.5:0.5 occupancy. H atoms were inserted in calculated positions and refined with a riding model. The following computer programs and hardware were used: structure solution, SHELXS-2014 and refinement, SHELXL-2014;[17] molecular diagrams, ORTEP;[18] computer, IntelCoreDuo. CCDC: 2263681, 2263682 and 2263683 for **1**·H_2O, **2**·CH_2Cl_2·0.5H_2O and **4**·$CHCl_3$, respectively.

Magnetic measurements

Dc magnetic susceptibility data (2–300 K) were collected on powdered samples using a SQUID magnetometer (Quantum Design MPMS-XL), applying a magnetic field of 0.1 T. All data were corrected for the contribution of the sample holder and the diamagnetism of the samples estimated from Pascal's constants.[19,20] The Mössbauer spectra were recorded on an alternating constant-acceleration spectrometer. The sample temperature was maintained constant in an Oxford Variox cryostat. The ^{57}Co/Rh source (1.8 GBq) was positioned at room temperature inside the gap of the magnet system at a zero-field position. Isomer shifts are referenced relative to iron metal at 295 K.

Electrochemistry

Cyclic voltammetric experiments with 0.5 mM solutions of investigated samples in 0.1 M *n*-Bu_4NPF_6 (p.a. quality from Fluka) supporting electrolyte in acetonitrile (p.a. quality from Sigma–Aldrich) were performed under argon atmosphere using a three-electrode arrangement with a platinum disk working electrode (from Ionode, Australia), platinum wire as a counter electrode, and silver wire as a pseudo reference electrode. All potentials in voltammetric studies were quoted vs ferricenium/ferrocene (Fc^+/Fc) redox couple. A Heka PG310USB (Lambrecht, Germany) potentiostat with a PotMaster 2.73 software package served for the potential control in voltammetric studies.

RESULTS AND DISCUSSION

Synthesis

Transmetallation reaction (Scheme 2) of $[ZnLIBa(CF_3SO_3)(CH_3OH)]_2\cdot 0.5H_2O$[11] with excess $FeCl_3\cdot 6H_2O$ in boiling methanol afforded the complex $[Fe^{III}LClBa(CH_3OH)(H_2O)_{0.5}\ (ZnCl_4)]\cdot$(**1**) crystallized as brown-black crystals of X-ray diffraction quality upon slow cooling of the reaction mixture in 64 % yield. Treatment of solution of **1** in CH_2Cl_2 with an aqueous solution of guanidinium sulfate resulted in the complex $[Fe^{III}LCl]$ (**2**) in 82 % yield. Metathesis reaction of 2 with excess NaN_3 in methanol afforded $[Fe^{III}L(N_3)]$ (**3**) in 94 % yield. The red solution obtained from the reaction of green-brown solution of **2** in methanol with air oxygen in the presence of triethylamine produced the μ_3-oxido-dimeric complex $[(Fe^{III}L)_2O]$ (**4**) in 79 % yield. The same complex **4** was synthesized from **2** when treated with KOH in water/$CHCl_3$.

*Characterization of **1**–**4***

Positive ion ESI mass spectrum of **1** showed a peak with *m*/*z* 513, which was assigned to $[Fe^{III}L]^+$, while the negative ion spectrum revealed a peak with *m/z* 169 attributed to $[ZnCl_3]^-$. The FAB mass spectrum displayed three peaks in the positive ion mode with *m/z* 720, 685 and 571. Their isotopic patterns were in agreement with theoretical isotopic distributions for $[Fe^{III}LBaCl_2–H]^+$, $[Fe^{III}LBaCl–H^+]^+$ and $[Fe^{III}LCl+Na^+]^+$, respectively. Like **1**, complexes **2** and **3** revealed in the ESI mass spectra a peak with *m*/*z* 513 due to $[Fe^{III}L]^+$ ion. A

strong stretching vibration at 2034 cm^{-1} in the IR spectrum of $[FeL(N_3)]$ indicated the presence of azide co-ligand in the complex.

In the positive ion ESI mass spectrum of **4** peaks at *m*/z 1081, 1065 and 1043 were assigned to $[(FeL)_2O+K^+]^+$, $[(FeL)_2O+Na^+]^+$ and $[(FeL)_2O+H^+]^+$, respectively. The band at 840 cm^{-1} in IR spectrum is due to asymmetric Fe–O–Fe stretching vibration.

$[ZnLIBa(CF_3SO_3)CH_3OH]$

↓(i)

$[Fe^{III}LClBa(CH_3OH)(H_2O)_{0.5}(ZnCl_4)]$ (**1**)

↓(ii)

$[Fe^{III}LCl]$ (**2**) —(iv)→ $[(Fe^{III}L)_2O]$ (**4**)

↓(iii)

$[Fe^{III}L(N_3)]$ (**3**)

Scheme 2. Synthesis of complexes **1**–**4**; Reaction conditions: i) $FeCl_3 \cdot 6H_2O$, CH_3OH; ii) guanidinium sulfate, CH_2Cl_2/H_2O 3:2; iii) NaN_3 (excess), CH_3OH; iv) Et_3N, CH_3OH or KOH, CH_2Cl_2/H_2O.

X-ray crystallography

The results of X-ray diffraction studies of complexes **1**, **2** and **4** are shown in Figs. 1–3 with pertinent metrical parameters in Table S-I. The iron(III) in **1** is five-coordinate with square-pyramidal coordination geometry. The ligand coordinates to iron(III) through two nitrogen atoms N1 and N3 of the isothiosemicarbazide moiety and two phenolato oxygen atoms O1 and O2 in the basal plane, while chlorido co-ligand Cl1 occupies the apical position. The iron(III) comes

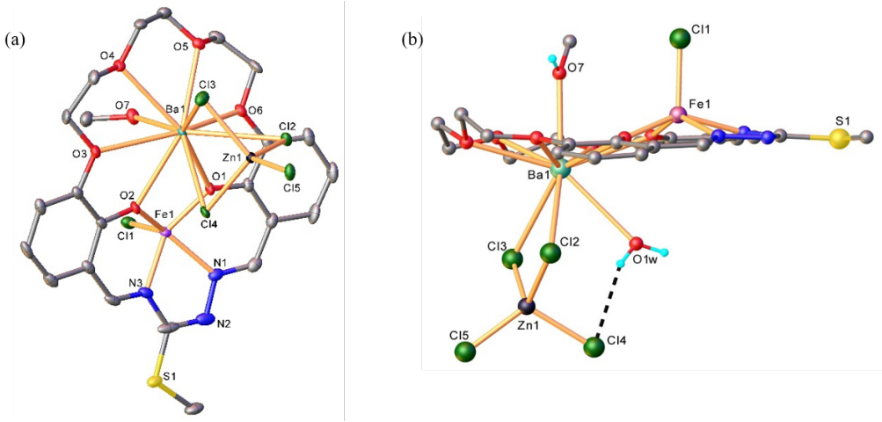

Fig. 1. a) ORTEP view of $[Fe^{III}LClBa(CH_3OH)(ZnCl_4)]$ with thermal ellipsoids at 50 % probability level and b) ball-and-stick representation of the second resolved counterpart of $[Fe^{III}LClBa(CH_3OH)(H_2O)_{0.5}(ZnCl_4)]$ in the crystal of $\mathbf{1} \cdot H_2O$. Interstitial solvent was removed for clarity.

out from the basal plane towards Cl1 by 0.612(2) Å. The metrical parameters are very close to those reported for iron(III) complex with bis(salicylidene)isothiosemicarbazide.[21] The Ba atom is 10-coordinate, with all six oxygen atoms of the macrocycle linked to the barium(II). The tetrahedral $[ZnCl_4]^{2-}$, which is disordered over two positions, forms three (Fig. 1a) and two bonding contacts to barium(II) through the chloride ions (Fig. 1b). When only two chlorido co-ligands are coordinated to the barium atom, an additional coordination of H_2O molecule is found (Fig. 1b). The molecule of CH_3OH is coordinated to the barium(II) on the other side of the macrocycle. The Ba^{2+} is displaced from the mean plane formed by the oxygen atoms of the crown ether moiety in opposite direction with that of iron(III) by 0.819(1) Å due to stronger interactions with $ZnCl_4^{2-}$ than with methanol molecule as shown in Fig. 1.

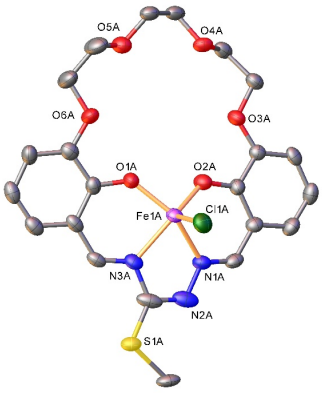

Fig. 2. ORTEP view of one of the two crystallographically independent molecules of $[Fe^{III}LCl]$ (**2**) with thermal ellipsoids at 50 % probability level. Interstitial solvent is not shown for clarity.

As expected square-pyramidal coordination geometry around Fe(III) was disclosed in complex **2**. The bi-compartmental ligand is bound to iron(III) through two nitrogen atoms N1 and N3 of the isothiosemicarbazide moiety and two phenolato oxygen atoms O1 and O2 in the basal plane, while the chlorido co-ligand Cl1 occupies the apical position. The iron(III) comes out from the basal plane towards Cl1 by 0.547(2) and 0.559(2) Å for the two crystallographically independent molecules A and B, respectively. The bond lengths around Fe(III) are very close to those in complex **1** and complex **5** (Table II).

The SC-XRD structure of **4** revealed that the two iron(III) ions with a square-pyramidal coordination environment N_2O_3 are associated into a dimer *via* a bridging oxido anion, O^{2-}. The angle Fe1−O1−Fe2 of 154.57(12)° is determined by steric repulsions between the two bi-compartmental ligands and is much higher than the angle of 139° reported as minimal for documented in the literature μ-oxido-bridged iron(III) complexes.[22]

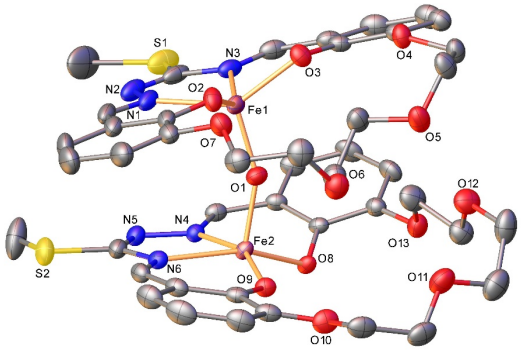

Fig. 3. ORTEP view of the μ_3-oxido-dimeric iron(III) complex $[(Fe^{III}L)_2O]$ **(4)**. Interstitial solvent was omitted for clarity.

TABLE II. Selected bond distances (Å) in the coordination polyhedron of Fe(III) in complexes **1**, **2** and **5**

Bond	Compound			
	1	**2**		**5**[a]
		Molecule A	Molecule B	
Fe–Cl1	2.1981(15)	2.2280(15)	2.2215(15)	2.212(2)
Fe–N1	2.085(5)	2.091(4)	2.086(4)	2.084(5)
Fe–N3	2.065(5)	2.075(4)	2.082(4)	2.101(4)
Fe–O1	1.899(4)	1.880(3)	1.882(4)	1.875(4)
Fe–O2	1.915(4)	1.879(3)	1.875(4)	1.894(4)

[a]Iron(III) complex with *S*-methyl-bis(salicylidene)isothiosemicarbazide (**5**) is reported in ref. 21

The dimeric complexes $[(Fe^{III}L)_2O]$ form centrosymmetric tetranuclear associates bridged *via* μ-phenolato oxygen atoms O8 and O8^i as shown in Fig. 4 with bond distances Fe2–O8 of 1.9463(17) Å and Fe2–O8^i of 2.4713(18) Å, ∠O8–Fe2–O8^i = 75.56(7)° and ∠Fe2–O8^i–Fe2^i = 104.44(7)° (symmetry code i: $1 - x$, $2 - y$, $1 - z$).

The optical spectra of **1**–**4** in methanol are shown in Fig. 5. The spectra are dominated by charge-transfer and intra-ligand transitions.

Magnetism and Mössbauer spectra

The variable temperature (*VT*) magnetic susceptibility measurement for complex **1** is shown in Fig. 6 as plots of χ_M vs. T and μ_{eff} *vs.* T, while the Mössbauer spectrum at 80 K is displayed in Fig. 7.

The magnetic susceptibility values for **1** at room temperature are of the order expected for the high-spin Fe(III) (S = 5/2) (5.98 μ_B or 4.465 cm^3 K mol^{-1}) at 300 K assuming g = 2.0, theoretical $\chi_M T$ value of 4.377 cm^3 K mol^{-1}.[20] The values of the magnetic susceptibility remain almost constant up to 50 K, after

which a progressive decrease of the magnetic susceptibility up to 2 K was seen, where the magnetic susceptibility value of 3.544 μ_B is reached.

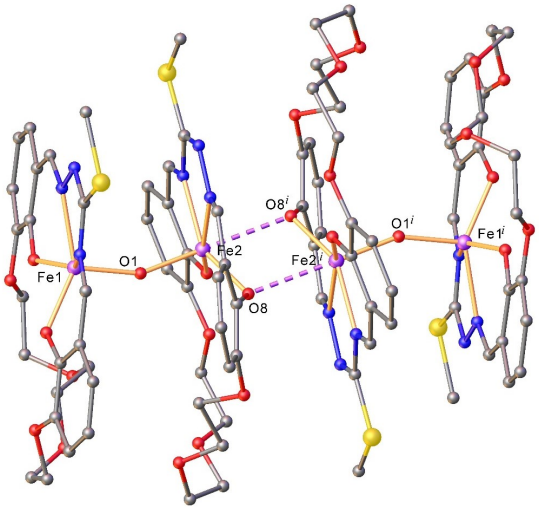

Fig. 4. Pairwise association of μ_3-oxido dimeric iron(III) complexes **4**.

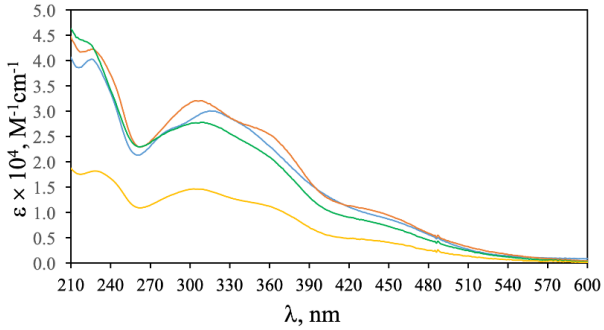

Fig. 5. The electronic spectra of methanolic solutions of **1** (red trace), **2** (blue trace), **3** (green trace) and **4** (yellow trace).

For an octahedral mononuclear high-spin iron(III) complex the ground state is $^6A_{1g}$ and the expected spin-only magnetic moment is 5.92 μ_B, which is temperature independent. However, if the symmetry is lowered, the $^6A_{1g}$ term can split to a small extent by mixing in, *via* spin-orbit coupling, the components of a higher-lying $^6T_1$ term.[23] Under symmetry lowering, some departure of the magnetic moment from the spin-only value and from Curie law behavior might be expected. Also, if there were any significant antiferromagnetic exchange interaction between the iron atoms in the crystal, the magnetic moment would be exp-

ected to decrease below the spin-only value and also to show an appreciable temperature dependence.[24]

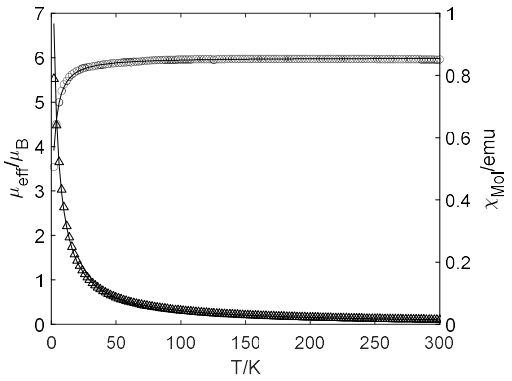

Fig. 6. The temperature dependence of the effective magnetic moment μ_{eff} and molar magnetic susceptibility for **1**.

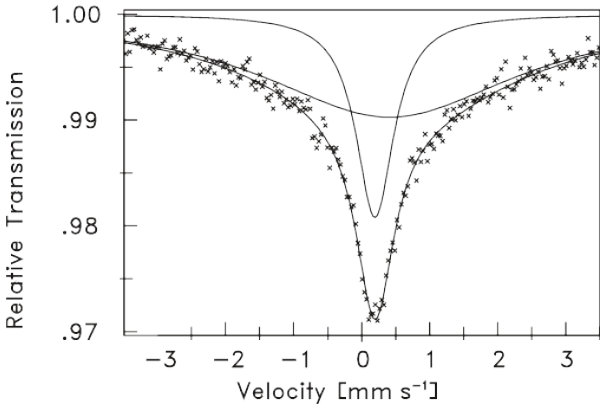

Fig. 7. Mössbauer spectrum of complex **1** at 80 K.

A series of Fe(salen)X complexes with magnetic moments in the range 5.7––6.0 μ_B at room temperature obeyed the Curie–Weiss law with small values of θ. The *VT* magnetic susceptibilities indicated that there was no significant magnetic exchange present. This result strongly suggested that those complexes were five-coordinate. In the case of nitromethane adduct of Fe(salen)Cl, X-ray diffraction analysis[25,26] revealed essentially square-pyramidal Fe(salen)Cl molecules, with the nitromethane molecule as interstitial solvent. At room temperature that compound had a magnetic moment close to the spin-only value for five unpaired electrons and the crystals also showed considerable magnetic anisotropy. This anisotropy arose from a zero-field splitting (ZFS) of the free-ion ^6S term, due to at least in part the low symmetry of the complex. Coordination of iron(III) com-

plex with a salen-crown bi-compartmental macrocycle to Ba^{2+} was reported previously and did not cause a change in the spin state of iron(III) in the solid state.[27]

Based on the structural data, the magnetic behavior of **1** was explained by the presence of anisotropy caused by ZFS, which will be also discussed in the Mössbauer study, as well as by a small intermolecular interaction (*zJ*). The following Hamiltonian was applied to model the magnetic susceptibility of **1**:[20]

$$\hat{H} = D\left(\vec{\hat{S}}_{z_i}^{\,2} - S(S+1)/3\right) + E\left(\vec{\hat{S}}_x^{\,2} - \vec{\hat{S}}_y^{\,2}\right) \quad (1)$$

Fitting the experimental data afforded the ZFS parameters: $D = 4.5(1)$ cm^{-1}; $E = 0.01(1)$ cm^{-1} and $g = 2.029(3)$ with intermolecular interaction $zJ = -0.11(1)$ cm^{-1}. Such values of the ZFS parameters were expected for square-pyramidal coordination geometry and are consistent with reported in the literature data for similar compounds.[28,29]

The Mössbauer spectrum of **1** (Fig. 7) was calculated as two broad singlets with isomeric shift (*I.S.*) *I.S.* 0.19 and 0.41 mm s^{-1} and full width at half maximum (*FWHM*) of 0.67 and 4.64 mm s^{-1}, respectively. The isomeric shifts are in agreement with high-spin iron(III) as also suggested from *VT* magnetic susceptibility measurements. Lack of quadrupole splitting indicates spherical symmetry of the iron(III) charge cloud in **1**.

The *I.S.* and quadrupole splitting (ΔE_Q) for complex **2** at 80 K (Fig. 8) are 0.43 and 0.94 mm/s and *FWHM* for both lines of the doublet line is 0.66 mm/s. These Mössbauer parameters are well comparable to that of iron complex with *S*-methyl-bis(salicylidene)isothiosemicarbazide[30] with *I.S.* of 0.50 mm/s and $\Delta E_Q = 0.95$ mm/s and $(FWHM)_L$ 0.64 mm s^{-1} and $(FWHM)_R$ 1.16±0.03 mm s^{-1} referred to iron foil and indicate high-spin Fe(III) ($S = 5/2$). The main feature of the Mössbauer spectrum of **2** and those of $Fe^{III}QCl$, where H_2Q = *S*-methyl-bis-(salicylidene)isothiosemicarbazide is their asymmetry, which was found temperature-dependent for iron(III) complex with *S*-methyl-bis(salicylidene)isothiosemicarbazide. The intensity of the two absorption peaks of the Mössbauer spectra of this latter complex was shown to be equalized at 4.2 K. The observed asymmetry of the Mössbauer spectra is likely due to spin-orbit coupling, which removes Zeeman degeneracy of the ground state ^6S into three Kramer's doublets, and different spin relaxation rates for the level ±1/2 and for ±3/2 and ±5/2.[25,31] This degeneration can be characterized in the first approximation with terms of ZFS (*D* and *E*) based on the Hamiltonian used for the description of magnetism. Similar spectroscopic behavior was also reported for iron(III) complexes with porphyrins.[28]

Somewhat different ΔE_Q values to those for high-spin octahedral and five-coordinate iron(III) complexes with thiosemicarbazones[32,33] are likely due to difference in population of d_{x2-y2}, d_{xy}-orbitals from one side, and d_{z2}, d_{xz}, d_{yz}-orb-

itals from the other side, because of different ligand identity and coordination geometry of iron(III). The total s-electron density on the nucleus remained unchanged, while the quadrupole splitting markedly differed.

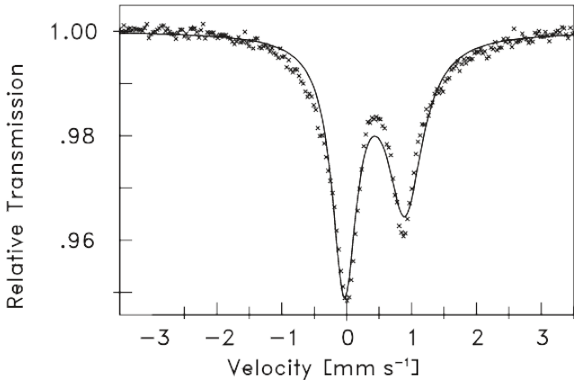

Fig. 8. Mössbauer spectrum of complex **2** at 80 K.

The Mössbauer spectrum of complex **3** (Fig. 9) revealed a doublet with almost equal intensity of both lines already at 80 K. The *I.S.* and ΔE_Q of 0.42 and 0.74 mm s^{-1} respectively, and *FWHM* of 0.35 mm s^{-1} are close to the Mössbauer parameters for complex **2** and in agreement with high-spin configuration of Fe(III).

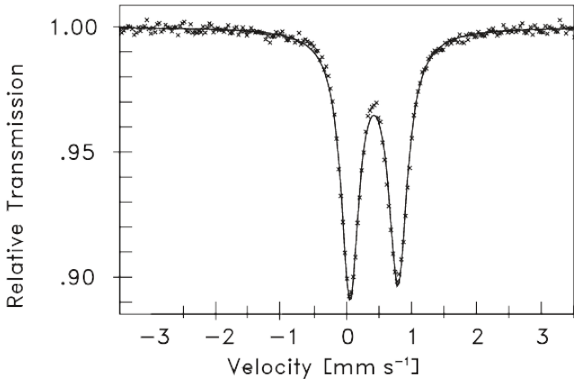

Fig. 9. Mössbauer spectrum of **3** at 80 K.

The departure of the iron(III) charge cloud from spherical symmetry of the free iron(III) ion is higher in complex **2** with chlorido apical ligand (ΔE_Q = 0.94 mm s^{-1}) than in complex **3** with azide as co-ligand (ΔE_Q = 0.74 mm s^{-1}). The same picture was disclosed previously for iron(III) porphyrin complexes.[28]

The magnetic measurement for complex **4** showed an expected, for dimeric μ-oxido-bridged iron(III) complexes, temperature dependence (Fig. 10). The

effective magnetic moment was of 2.65 μ_B (0.875 cm^3 K mol^{-1}) at 300 K and decreased steadily up to 0.6 μ_B at 2 K. This behavior indicated a strong antiferromagnetic interaction between the two high-spin iron(III) centers. From this interaction resulted a spin ground state $S_T = 0$. The low temperature curve indicated the presence of temperature independent paramagnetism (TIP). The fitting procedure gave a coupling constant $J = -113.1$ cm^{-1} ($H = -2JS_1 \cdot S_2$, $g = 2.0$ fixed parameter) and *TIP* of 496×10^{-6} cm^3 mol^{-1} per dimer.

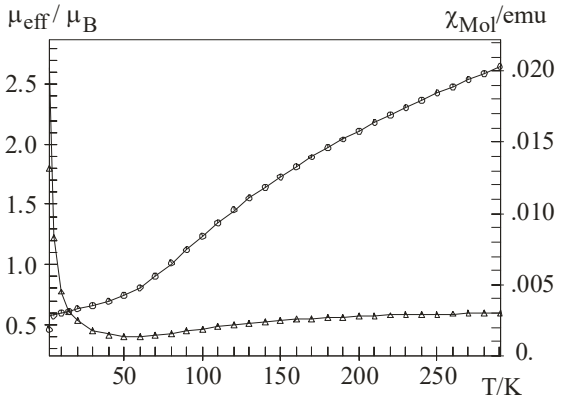

Fig. 10. The *VT* effective magnetic moment μ_{eff} and *VT* molar magnetic susceptibility for di-iron(III) complex **4**.

The strong antiferromagnetic Fe–Fe interaction with a similar magnitude of –115.3 cm^{-1} was reported for μ-oxido di-Fe(III) complex with 1,2-bis((3-methoxysalicylidene)amino)ethane[34] and other μ-oxido-bridged diiron(III) complexes and falls in the range of those calculated from empirical correlation equations considering the average Fe–O bond within the μ-oxido bridge.[35]

Electrochemical studies

The electrochemical behavior of **1**–**4** in MeCN was studied by cyclic voltammetry. The cyclic voltammogram of [Fe^{III}LCl] (**2**) in MeCN/*n*-Bu_4NPF_6 at Pt working electrode at scan rate of 100 mV s^{-1} showed in the cathodic region a quasireversible reduction with cathodic half-wave potential $E_{1/2} = -0.64$ V *vs*. Fc^+/Fc^0 (Fig. 11a). This event was attributed to the one-electron reversible reduction of Fe(III) to Fe(II). At more negative potentials new redox processes were identified in the range from –1.2 to –1.4 V *vs*. Fc^+/Fc^0, which were likely due to the ligand reduction. Coordination of iron(III) complex *via* its crown ether moiety to Ba^{2+} led to a shift of the first reduction step for **1** to the less negative value of –0.41 V *vs*. Fc^+/Fc^0 when compared to **2** indicating a quite strong effect of Ba^{2+} binding to the macrocycle on the redox behavior of Fe(III) (Fig. 11b). The second nearly irreversible reduction step took place at $E_{pc} = -1.68$ V *vs*.

Fc^+/Fc^0. Replacement of the chlorido co-ligand by azide (N_3^-) co-ligand afforded a slight shift of the cathodic half-wave potential for **3** ($E_{1/2}$ = –0.67 V *vs*. Fc^+/Fc^0) when compared to **2**. The second nearly irreversible cathodic peak for **3** was seen at E_{pc} = –1.1 V *vs*. Fc^+/Fc^0. For the dimeric μ-oxido bridged iron(III) complex [$(Fe^{III}L)_2O$] (**4**) a more complex redox behavior in the cathodic part was observed (Fig. 12).

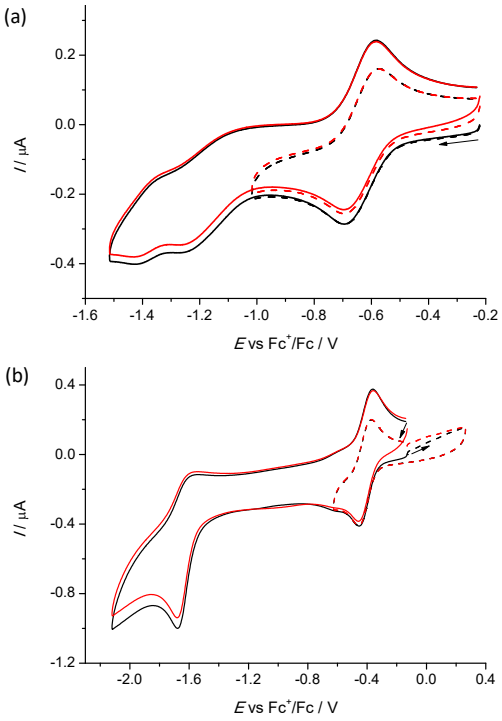

Fig. 11. Cyclic voltammetry of: a) [$Fe^{III}LCl$] (**2**) and b) complex **1** in MeCN/*n*-Bu_4NPF_6 at Pt working electrode (scan rate 100 mV s^{-1}, black trace – the first scan, red trace – the second scan, dashed lines – reduction to the first redox event).

The corresponding cyclic voltammogram showed the first reduction peak at E_{pc} = –1.29 V *vs.* Fc^+/Fc^0 with a strongly shifted reoxidation peak at –0.54 V exhibiting typical features of either a slow electron process or electrochemical square scheme. We suggest that a strongly shifted reoxidation peak upon reverse scan was due to a significant rearrangement of the dimeric complex after one electron reduction of one Fe(III) center in the dimer to Fe(II). Note that no oxidation process was observed in the range from –0.1 to 0.3 V just going to the anodic region before starting the reduction. The second reduction peak at E_{pc} = = –1.50 V *vs.* Fc^+/Fc^0 showed reversible behavior and was tentatively ascribed to the reduction of the second Fe(III) in the dimer at a slightly more negative potential compared to the first reduction event. Additionally, a further quasirev-

ersible, likely ligand-based, reduction at more negative potential (E_{pc} = –2.0 V *vs*. Fc^+/Fc^0) was found. Generally the dimeric μ-oxido-bridged iron(III) complex exhibited more negative redox potentials compared to those of the monomeric counterparts. No oxidation processes were observed in the range from –0.4 to +0.4 V vs Fc^+/Fc^0 when going to the anodic region.

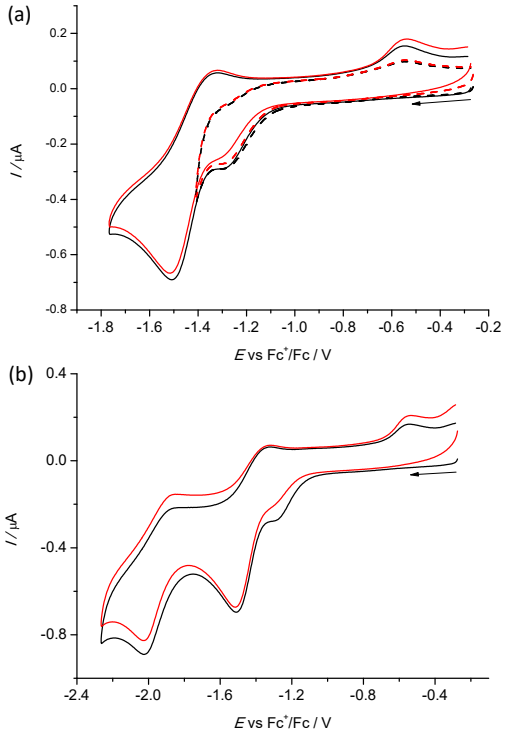

Fig. 12. a) Cyclic voltammetry of dimeric μ-oxido-bridged iron(III) complex $[(Fe^{III}L)]_2O]$ (**4**) in MeCN/*n*-Bu_4NPF_6 at Pt working electrode (scan rate 100 mV s^{-1}, black traces – the first scan, red traces – the second scan, dashed lines – reduction to the first redox event); b) cathodic reduction of **4** when going to the more negative potentials.

CONCLUSION

Transmetallation reaction of $[ZnLIBa(CF_3SO_3)(CH_3OH)]_2$ with excess $FeCl_3 \cdot 6H_2O$ in methanol afforded the high-spin iron(III)–barium(II)–zinc(II) complex **1**. Accommodation of barium(II) in the crown-ether moiety and coordination of tetrahedral dication $[ZnCl_4]^{2-}$ *via* three chlorido co-ligands (face) or via two chlorido ligands (edge) resulted in spherical symmetry of the iron(III) charge cloud as implied from the lack of quadrupole splitting in Mössbauer spectrum. Demetallation of crown-ether moiety by treatment of **1** with guanidinium sulfate afforded the mononuclear high-spin iron(III) complex $[Fe^{III}LCl]$ (**2**), which was further converted by metathesis reaction into $[Fe^{III}L(N_3)]$ (**3**). Like in **1**, the iron(III) in **2** and **3** adopts high-spin electronic configuration and square-pyramidal coordination geometry. In contrast to **1**, complexes **2** and **3** show a

quadrupole doublet in Mössbauer spectra at 80 K. The doublet asymmetry, which was more obvious in the spectrum of **2**, was likely due to spin-orbit coupling of the ground state ^6S into three Kramer's doublets and different spin relaxation rates for the level ±1/2 and for ±3/2 and ±5/2 as was also observed in five-coordinate iron(III) complexes with porphyrins. Complexes **2** and **3** in the presence of a strong base were found to form the μ-oxido-dimeric iron(III) complex $[(Fe^{III}L)_2O]$ (**4**). The *VT* magnetic measurements for **4** indicated strong antiferromagnetic interaction between two high-spin iron(III) centers and a spin ground state $S_T = 0$. Cyclic voltammograms showed that complexes **1**–**3** can be quasireversible reduced by one-electron at iron center. The $E_{1/2}$ reduction potential follows the order: **1 > 2 > 3**. The μ-oxido diiron(III) complex can be reduced stepwise at more negative potentials (–1.29 and –1.50 V) compared to those for mononuclear compounds (–0.41 V for **1**, –0.64 V for **2** and –0.67 V for **3**) indicating marked electrochemical communication between the two iron centers in **4**.

SUPPLEMENTARY MATERIAL

Additional data and information are available electronically at the pages of journal website: https://www.shd-pub.org.rs/index.php/JSCS/article/view/9813, or from the corresponding author on request. CIFs are available from the corresponding author on request.

Acknowledgements. VBA thanks the Austrian Science Fund for the support of the present work via grant no. I4729. We thank Dr. Richard Goddard for collection of X-ray diffraction data. PR thanks the Slovak Grant Agency APVV (grant APVV-19-0024) and the Operational Program Integrated Infrastructure for the project: "Support of research activities of Excellence laboratories STU in Bratislava", Project no. 313021BXZ1, co-financed by the European Regional Development Fund, for the financial support. OP thanks National Agency for Research and Development of the Republic of Moldova, grant 20.80009.5007.12. We thank Manuela Gross for the synthesis of X-ray diffraction quality single crystals of complex **4**.

ИЗВОД

КОМПЛЕКСИ ГВОЖЂА(III) СА ДИТОПИЈСКИМ МАКРОЦИКЛИКЛИМА КОЈИ САДРЖЕ КРУНА-ЕСТАРСКИ И БИС(САЛИЦИЛИДЕН)-ИЗОТИОСЕМИКАРБАЗИДНИ ОСТАТАК

VLADIMIR B. ARION[1], OLEG PALAMARCIUC[2], SERGIU SHOVA[3], GHENADIE NOVITCHI[4] и PETER RAPTA[5]

[1]University of Vienna, Institute of Inorganic Chemistry, Währinger Strasse 42, A-1090 Vienna, Austria, [2]Moldova State University, A. Mateevici Street 60, MD-2009 Chisinau, Republic of Moldova, [3]Inorganic Polymers Department, "Petru Poni" Institute of Macromolecular Chemistry, Aleea Gr. Ghica Voda 41 A, Iasi 700487, Romania, [4]CNRS-LNCMI, 38042 Grenoble Cedex, France и [5]Institute of Physical Chemistry and Chemical Physics, Faculty of Chemical and Food Technology, Slovak University of Technology in Bratislava, Radlinského 9, SK-81237 Bratislava, Slovakia

Главни циљеви рада били су синтеза и карактеризација комплекса гвожђа(III) са дитопијским лигандом H_2L који се састоји од бис(салицилиден)изотиосемикарбазидног остатка са N_2O_2 донорским сетом и круна-етарског остатка са O_6 донорским сетом атома. Синтетисана су четири високоспинска комплекса гвожђа(III) формула $[Fe^{III}LClBa(CH_3OH)(H_2O)_{0.5}(ZnCl_4)]$ (**1**), $[Fe^{III}LCl]$ (**2**), $[Fe^{III}L(N_3)]$ (**3**) и $[(Fe^{III}L)_2O]$ (**4**). Комплекси су окарактерисани масеном спектрометријом, IR и UV–Vis спектроско-

пијом, мерењима магнетне сусцептибилности при варијабилној температури, Mössbauer спектроскопијом, дифракцијом рендгенских зрака на монокристалу и цикличном волтаметријом.

(Примљено 7. јуна, ревидирано 4. јула, прихваћено 8. септембра 2023)

REFERENCES

1. C. J. Van Staveren, J. Van Eerden, F. C. J. M. Van Veggel, S. Harkema, D. N. Reinhoudt, *J. Am. Chem. Soc.* **110** (1988) 4994 (https://doi.org/10.1021/ja00223a017)
2. F. C. J. M. Van Veggel, S. Harkema, M. Bos, W. Verboom, C. J. Van Staveren, G. J. Gerritsma, D. N. Reinhoudt, *Inorg. Chem.* **28** (1989) 1133 (https://doi.org/10.1021/ic00305a025)
3. F. C. J. M. van Veggel, W. Verboom, D. N. Reinhoudt, *Chem. Rev.* **94** (1994) 279 (https://doi.org/10.1021/cr00026a001)
4. D. N. Reinhoudt, A. R. Van Doorn, W. Verboom, *J. Coord. Chem.* **27** (1992) 91 (https://doi.org/10.1080/00958979209407946)
5. C. J. Van Staveren, D. E. Fenton, D. N. Reinhoudt, J. Van Eerden, S. Harkema, *J. Am. Chem. Soc.* **109** (1987) 3456 (https://doi.org/10.1021/ja00245a045)
6. C. J. van Staveren, D. N. Reinhoudt, J. van Eerden, S. Harkema, *J. Chem. Soc., Chem. Commun.* (1987) 974 (https://doi.org/10.1039/c39870000974)
7. D. M. Rudkevich, W. P. R. V. Stauthamer, W. Verboom, J. F. J. Engbersen, S. Harkema, D. N. Reinhoudt, *J. Am. Chem. Soc.* **114** (1992) 9671 (https://doi.org/10.1021/ja00050a064)
8. J. Halfpenny, R. W. H. Small, *J. Chem. Soc., Chem. Commun.* (1979) 879 (https://doi.org/10.1039/c39790000879)
9. V. B. Arion, V. C. Kravtsov, J. I. Gradinaru, Yu. A. Simonov, N. V. Gerbeleu, J. Lipkowski, J.-P. Wignacourt, H. Vezin, O. Mentré, *Inorg. Chim. Acta* **328** (2002) 123 (https://doi.org/10.1016/S0020-1693(01)00717-4)
10. M. T. Reetz, V. B. Arion, R. Goddard, Y. A. Simonov, V. Ch. Kravtsov, J. Lipkowski, *Inorg. Chim. Acta* **238** (1995) 23 (https://doi.org/10.1016/0020-1693(95)04661-R)
11. V. B. Arion, E. Bill, M. T. Reetz, R. Goddard, D. Stöckigt, M. Massau, V. Levitsky, *Inorg. Chim. Acta* **282** (1998) 61 (https://doi.org/10.1016/S0020-1693(98)00198-4)
12. V. B. Arion, J. P. Wignacourt, P. Conflant, M. Drache, M. Lagrenee, O. Cousin, H. Vezin, G. Ricart, W. Joppek, H.-W. Klein, *Inorg. Chim. Acta* **303** (2000) 228 (https://doi.org/10.1016/S0020-1693(00)00038-4)
13. V. B. Arion, V. C. Kravtsov, R. Goddard, E. Bill, J. I. Gradinaru, N. V. Gerbeleu, V. Levitschi, H. Vezin, Y. A. Simonov, J. Lipkowski, V. K. Bel'skii, *Inorg. Chim. Acta* **317** (2001) 33 (https://doi.org/10.1016/S0164-1212(00)00107-2)
14. J. Costes, F. Dahan, G. Novitchi, V. Arion, S. Shova, J. Lipkowski, *Eur. J. Inorg. Chem.* (2004) 1530 (https://doi.org/10.1002/ejic.200300486)
15. M. T. Reetz, V. B. Arion, R. Trültzsch, H. Buschmann, E. Cleve, *Chem. Ber.* **128** (1995) 1089 (https://doi.org/10.1002/cber.19951281106)
16. J.-C. Moutet, E. Saint-Aman, E.-M. Ungureanu, V. Arion, N. Gerbeleu, M. Revenco, *Electrochim. Acta* **46** (2001) 2733 (https://doi.org/10.1016/S0013-4686(01)00482-0)
17. G. M. Sheldrick, *Acta Crystallogr., A* **64** (2008) 112 (https://doi.org/10.1107/S0108767307043930)
18. M. N. Burnett,C. K. Johnson, *ORTEP-III: Oak Ridge Thermal Ellipsoid Plot Program for Crystal Structure Illustrations*, Oak Ridge National Laboratory, Oak Ridge, TN, 1996 (https://doi.org/10.2172/369685)

19. G. A. Bain, J. F. Berry, *J. Chem. Educ.* **85** (2008) 532 (https://doi.org/10.1021/ed085p532)
20. O. Kahn, *Molecular Magnetism*, Wiley-VCH, New York, 1993 (ISBN 0471188787, 9780471188384)
21. M. A. Yampol'skaya, S. G. Shova, N. V. Gerbeleu, V. K. Bel'skii, Yu. A. Simonov, *Zh. Neorg. Khim.* **27** (1982) 2551
22. K. S. Murray, *Coord. Chem. Rev.* **12** (1974) 1 (https://doi.org/10.1016/S0010-8545(00)80384-7)
23. J. S. Griffith, *Mol. Phys.* **8** (1964) 213 (https://doi.org/10.1080/00268976400100251)
24. M. Gerloch, J. Lewis, F. E. Mabbs, A. Richards, *J. Chem. Soc. A* (1968) 112 (https://doi.org/10.1039/J19680000112)
25. M. Gerloch, J. Lewis, F. E. Mabbs, A. Richards, *Nature* **212** (1966) 809 (https://doi.org/10.1038/212809a0)
26. M. Gerloch, F. E. Mabbs, *J. Chem. Soc., A* (1967) 1598 (https://doi.org/10.1039/J19670001598)
27. S. Hayami, S. Nomiyama, S. Hirose, Y. Yano, S. Osaki, Y. Maeda, *J. Radioanal. Nucl. Chem*. **239** (1999) 273 (https://doi.org/10.1007/BF02349496)
28. T. H. Moss, A. J. Bearden, W. S. Caughey, *J. Chem. Phys.* **51** (1969) 2624 (https://doi.org/10.1063/1.1672387)
29. G. Feher, P. L. Richards, in *Magnetic Resonance in Biological Systems*, Elsevier, Amsterdam, 1967, pp. 141−144 (https://doi.org/10.1016/B978-1-4832-1333-0.50019-7)
30. S. G. Shova, M. A. Yampol'skaya, B. G. Zemskov, N. V. Gerbeleu, K. I. Turta, I. N. Ivleva, *Zh. Neorg. Khim.* **30** (1985) 2309
31. M. Blume, *Phys. Rev. Lett.* **18** (1967) 305 (https://doi.org/10.1103/PhysRevLett.18.305)
32. A. V. Ablov, V. I. Gol'danskii, K. I. Turta, R. A. Stukan, V. V. Zelentsov, E. V. Ivanov, N. V. Gerbeleu, *Dokl. Akad. Nauk SSSR* **196** (1971) 1101
33. N. V. Gerbeleu, K. I. Turta, V. M. Canic, V. M. Leovac, V. B. Arion, *Koord. Khim.* **6** (1980) 446
34. J.-P. Costes, F. Dahan, F. Dumestre, J. Modesto Clemente-Juan, J. Garcia-Tojal, J.-P. Tuchagues, *Dalton Trans.* (2003) 464 (https://doi.org/10.1039/b210950f)
35. S. M. Gorun, S. J. Lippard, *Inorg. Chem.* **30** (1991) 1625 (https://doi.org/10.1021/ic00007a038).